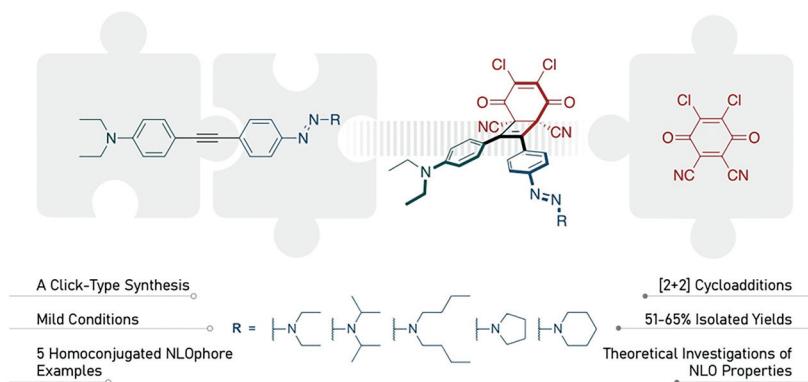


# Click-Type Synthesis of Homoconjugated Push–Pull Chromophores: Computational Investigation of Optical and Nonlinear Optical (NLO) Properties

Fevzi Can Inyurt  
Flora Mammadova  
Cagatay Dengiz\*

Department of Chemistry, Middle East Technical University,  
06800 Ankara, Turkey  
dengizc@metu.edu.tr

Published as part of the Virtual Collection  
*Click Chemistry and Drug Discovery*



Received: 07.12.2022  
Accepted after revision: 29.12.2022  
Published online: 29.12.2022 (Accepted Manuscript),  
24.01.2023 (Version of Record)  
DOI: 10.1055/a-2004-6344; Art ID: SO-2022-12-0069-OP



License terms:

© 2022. The Author(s). This is an open access article published by Thieme under the terms of the Creative Commons Attribution License, permitting unrestricted use, distribution and reproduction, so long as the original work is properly cited. (<https://creativecommons.org/licenses/by/4.0/>)

**Abstract** Homoconjugated push–pull chromophores were obtained by an efficient, click-type formal [2+2] cycloaddition. With these short synthetic transformations, complex chromophore structures were achieved in a single step without any by-product formation. Significant second-order optical nonlinearities have been calculated for the synthesized compounds.

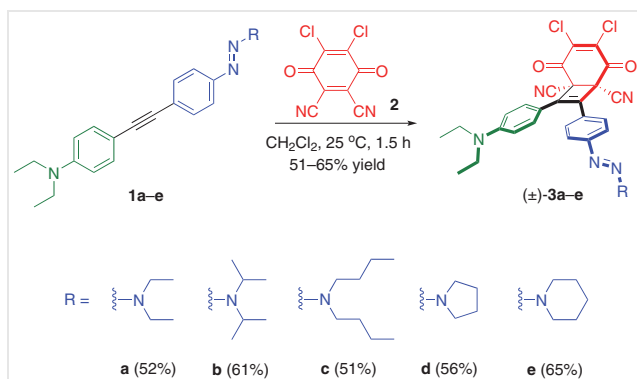
**Key words** triazene, nonlinear optics, [2+2] cycloaddition, homoconjugation, donor–acceptor systems, intramolecular charge transfer

The term ‘click chemistry’ was introduced by Sharpless and colleagues in 2001 and the developed concept earned the Nobel Prize in Chemistry in 2022.<sup>1</sup> The main argument behind this work was to develop reliable, nature-inspired reactions that could be used to synthesize molecules with desired properties. According to the proposal, chemical transformations must meet certain criteria in order to be defined as click reactions. Thus, click reactions must be selective, broad in scope, deliver very high yields, and only produce simple side products that may be eliminated using non-chromatographic techniques such as crystallization and distillation.<sup>1</sup> Although the most well-known example of these reactions is the azide-alkyne 1,3-dipolar cycloaddition,<sup>2,3</sup> many other transformations such as [4+2] and [2+2] cycloadditions,<sup>1</sup> [2+2] cycloaddition-retroelectrocycliza-

tions,<sup>4</sup> thiol-ene reactions,<sup>5,6</sup> and ring-opening reactions of strained heterocyclic electrophiles<sup>7</sup> are classified as click-type reactions. Recent studies have shown that click-type reactions such as [2+2] cycloadditions and [2+2] cycloaddition-retroelectrocyclizations are now frequently used in the synthesis of push–pull structures.<sup>4</sup> The excellent optoelectronic properties of these structures explain the growing interest in their synthesis by using short and efficient click-type methods. Push–pull systems also find applications in a wide variety of areas such as organic light-emitting diodes (OLEDs),<sup>8</sup> organic field-effect transistors (OFETs),<sup>9</sup> dye-sensitized solar cells (DSSCs),<sup>10</sup> and nonlinear optical (NLO) devices.<sup>11</sup> In this context, it is essential to develop efficient synthetic strategies to access these valuable targets. All the above-mentioned features make click-type transformations an excellent area to explore. As mentioned, the formal [2+2] cycloaddition is one of many examples of click chemistry and it can be applied successfully for the synthesis of push–pull chromophores. Although the Woodward–Hoffman rules<sup>12</sup> state that [2+2] cycloaddition under thermal conditions is unlikely, strong donor and withdrawal group insertions in starting materials may change the conventional perspective. In 1973, Reinhoudt reported the first example of a [2+2] cycloaddition between an electron-rich alkyne and electron-deficient alkene under thermal conditions.<sup>13</sup> This pioneering work was followed by many others and revealed many potential thermal [2+2] cycloaddition transformations.<sup>14,15</sup> Two of the more recent contributions in this field are the [2+2] cycloadditions between dialkylaniline/indole-based electron-rich alkynes and DDQ, which is well-known as an oxidant,<sup>16</sup> carried out independently by the Trofimov and Diederich groups.<sup>17,18</sup> In 2019, our group successfully demonstrated that triazenes can also be used

as donor groups in formal [2+2] cycloadditions.<sup>19</sup> Following this work, our attempts to broaden the scope of substrates that could be used in [2+2] cycloadditions with double triazene-substituted alkynes unfortunately did not work. To circumvent this issue, we have recently designed unsymmetrical dialkylaniline/triazene-substituted alkynes that undergo successful [2+2] cycloaddition-retroelectrocyclization to form  $\pi$ -conjugated non-planar push-pull NLOphores.<sup>11</sup> As part of our ongoing investigations on push-pull-type NLOphores, we herein present the synthesis of homoconjugated push-pull chromophores via click-type formal [2+2] cycloaddition.

The synthetic part of the study was divided into two parts: the synthesis of disubstituted alkynes **1a–e** and their [2+2] cycloadditions with DDQ (**2**) (Scheme 1). The synthesis of alkynes **1a–e** was carried out based on the literature, as described in detail in our previous work.<sup>11</sup> In summary, the synthesis of five electron-rich alkynes **1a–e** was performed using Sonogashira cross-coupling as the key step. With substrates **1a–e** in hand, subsequent click-type [2+2] cycloaddition reactions were tested. Upon mixing 1:1 stoichiometries of alkynes **1a–e** and DDQ (**2**), the target homoconjugated chromophores ( $\pm$ )-**3a–e** were obtained in 51–65% yield in less than 1.5 hours. In all cases, complete consumption of the starting material was confirmed by TLC analysis, and no by-product formation was observed. The reason for the moderate yields is presumably the difficulties encountered during isolation steps; during our purification attempts by column chromatography using silica gel or aluminum oxide (neutral or basic), slight degradation of the cycloadducts ( $\pm$ )-**3a–e** was observed.



**Scheme 1** Cycloadditions of disubstituted alkynes **1a–e** with DDQ (**2**)

Immediately after the isolation of the homoconjugated compounds ( $\pm$ )-**3a–e**, their optoelectronic properties were studied by UV/Vis spectroscopy, which is the most commonly used technique to investigate intramolecular charge-transfer (ICT) properties of such chromophores. In order to investigate the ICT behavior of ( $\pm$ )-**3a–e**, UV/Vis spectra were recorded in  $\text{CH}_2\text{Cl}_2$  at 25 °C. Accordingly, molar extinction coefficients of the lowest energy absorption bands range between 3300 and 8600  $\text{M}^{-1}\text{cm}^{-1}$  (Figure 1).

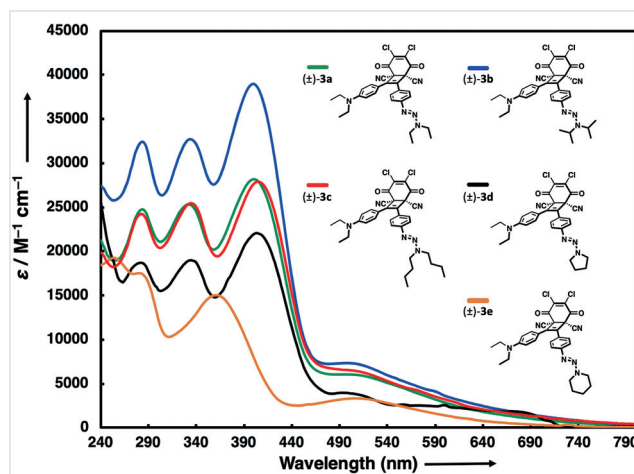


**Figure 1** UV/Vis absorption spectra of chromophores ( $\pm$ )-**3a** (green), ( $\pm$ )-**3b** (blue), ( $\pm$ )-**3c** (red), ( $\pm$ )-**3d** (black), ( $\pm$ )-**3e** (orange) in  $\text{CH}_2\text{Cl}_2$  at 298 K.

Cycloadducts ( $\pm$ )-**3a–e** show  $\lambda_{\text{max}}$  values ranging between 495 and 505 nm for the ICT bands;  $\lambda_{\text{max}} = 496$  nm (7300  $\text{M}^{-1}\text{cm}^{-1}$  for ( $\pm$ )-**3a**), 498 nm (8600  $\text{M}^{-1}\text{cm}^{-1}$  for ( $\pm$ )-**3b**), 496 nm (8300  $\text{M}^{-1}\text{cm}^{-1}$  for ( $\pm$ )-**3c**), 495 nm (3300  $\text{M}^{-1}\text{cm}^{-1}$  for ( $\pm$ )-**3d**), and 505 nm (5700  $\text{M}^{-1}\text{cm}^{-1}$  for ( $\pm$ )-**3e**). These results illustrate that different alkyl substitution on triazenes has no significant impact on  $\lambda_{\text{max}}$  values. In the next step, computational methods were used to verify whether the low-energy absorption bands observed in experimental UV/Vis measurements have ICT character or not. All calculations were carried out using the Gaussian 09 software package.<sup>20</sup> Geometry optimizations of ( $\pm$ )-**3a–e** were carried out at the CAM-B3LYP/6-31G\* level of theory.<sup>21</sup> The analysis of the analytical frequencies computed at the same level for cycloadducts ( $\pm$ )-**3a–e** confirmed that the structures are all at ground-state minima and none of them have imaginary frequencies. The conductor-like polarizable continuum model (CPCM) was applied as a solvation model in  $\text{CH}_2\text{Cl}_2$ .<sup>22</sup> To interpret and understand the experimental UV/Vis spectral features, we applied a TD-DFT [CAM-B3LYP/6-31G\*] approach as a tool for the calculation of ICT bands arising from homoconjugated donor–acceptor interactions.<sup>23</sup> As expected, the lowest-energy absorption bands were confirmed to correspond to HOMO→LUMO transitions. For all substrates, the calculated  $\lambda_{\text{max}}$  values (536–540 nm) are slightly larger than the experimental values (495–505 nm) (Tables 1SI–5SI). The small differences observed between the experimental and calculated spectra are consistent with those observed in similar D-A systems reported in the literature.<sup>24</sup> The frontier molecular orbital (FMO) depictions and electrostatic potential maps (ESP) were used to support further the ICT character of the lowest energy bands observed in experimental UV/Vis spectra.<sup>25</sup> Table 1 displays HOMO and LUMO depictions and ESP views from two different angles for the selected homoconjugated chromophore ( $\pm$ )-**3a**. The

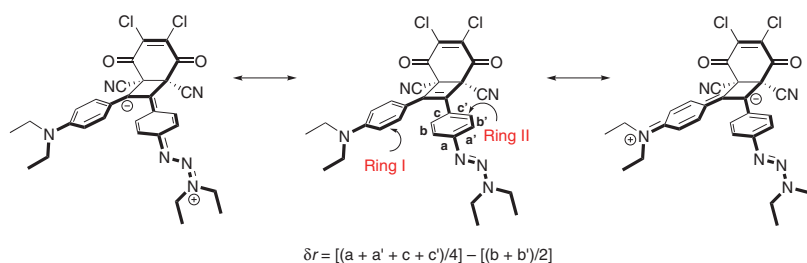
**Table 1** HOMO/LUMO Depictions and ESP Maps for Selected Chromophore ( $\pm$ )-**3a**

Structure	HOMO	LUMO	ESP (front view) <sup>a</sup>	ESP (side view) <sup>a</sup>
 ( $\pm$ )- <b>3a</b>				

<sup>a</sup> Mapped over the range  $-0.02$  a.u. (red) to  $0.02$  a.u. (blue)

topology of the frontier orbitals clearly confirms the ICT interactions. The HOMO is more concentrated on the electron-rich dialkyl aniline and triazene groups, while the LUMO is mainly located on the six-membered ring containing cyanide, carbonyl, and halogen groups. It is noteworthy that the HOMO is more concentrated on the dialkyl aniline, which is known to be a stronger donor group than a triazene. The small but significant overlap between HOMO and LUMO indicates successful charge transfer between the donor and the acceptor groups. ESP maps, as one of the most frequently employed visualization techniques to describe electron-transfer interactions in D-A systems, are also given in Table 1.<sup>25–27</sup> The regions shown in red represent the regions where the electron density increases after ICT and the regions shown in blue represent the regions where the electron density decreased. Accordingly, it is notable that the electron density is concentrated around the six-membered ring, in line with the FMO results.

The distinctive bond-length alternation arising from intramolecular charge-transfer interactions was accounted for both benzene rings (Rings I and II, Table 2) in homoconjugated structures ( $\pm$ )-**3a–e**. While the quinoid character value ( $\delta r$ ) is 0 for benzene, the  $\delta r$  value varies between 0.08 and 0.10 in systems with a fully quinoid structure.<sup>17</sup> The diethyl aniline rings in ( $\pm$ )-**3a–e** exhibit a  $\delta r$  value of 0.030, while the triazene substituted benzene rings have  $\delta r$  values of 0.017–0.018. The lack of difference between the  $\delta r$  values of rings I and II of the different chromophores is consistent with the UV/Vis measurements, indicating that the changes in the triazene groups have no effect on the optoelectronic properties. Additionally, the significant  $\delta r$  value differences observed between the two rings in the series of ( $\pm$ )-**3a–e** confirm that the diethyl aniline ring is a much stronger donor group than the triazenes. These results support the through-bond interactions being the dominant mechanism for formation of intramolecular charge-transfer transitions.

**Table 2** Calculated Quinoidal Character Values ( $\delta r$ ) of ( $\pm$ )-**3a–e**

Compound	$\delta r$ (Å)	
	Ring I	Ring II
( $\pm$ )- <b>3a</b>	0.030	0.018
( $\pm$ )- <b>3b</b>	0.030	0.018
( $\pm$ )- <b>3c</b>	0.030	0.018
( $\pm$ )- <b>3d</b>	0.030	0.018
( $\pm$ )- <b>3e</b>	0.030	0.017

The theoretical band gaps of homoconjugated chromophores ( $\pm$ )-**3a–e** are summarized in Figure 2. Band gaps ranging from 2.30 to 2.31 eV indicate once more that triazene derivatization has no significant impact on optoelectronic properties. The band gap results are also consistent with the experimental UV/Vis results.

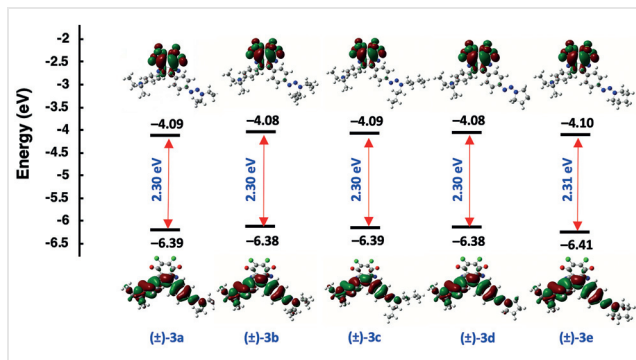


**Figure 2** Energy-level diagram of the frontier orbitals of push-pull dyes ( $\pm$ )-**3a–e** estimated by DFT calculations

Initial results obtained when the frontier orbitals were analysed showed that ( $\pm$ )-**3a–e** have the potential to possess NLO properties. Most of the NLOphores reported in the literature are constructed based on the donor- $\pi$ -spacer-acceptor (D- $\pi$ -A) structure.<sup>28,29</sup> In contrast, ( $\pm$ )-**3a–e** possess a D-A-D frame consisting of donor and acceptor groups that interact through a homoconjugated bridge. Limited studies on NLO properties of homoconjugated systems compared to the intensive research on  $\pi$ -conjugated structures motivated us to carry out theoretical NLO studies.<sup>17</sup> In general, NLOphores display strong ICT characteristics and NLO responses are directly proportional to the efficiency of ICT.<sup>25</sup> Since experimental measurement of NLO susceptibilities is expensive and rather challenging, we turned to quantum mechanical calculations incorporating DFT methods that are routinely used in NLO susceptibility calculations.<sup>11,30</sup>

Accordingly, various calculated parameters including average polarizability, first hyperpolarizability, dipole moment, band gap, electronegativity, global chemical hardness, and softness are listed in Table 3. The equations used to calculate these parameters, are given in Table 4.

**Table 4** Equations Used to Calculate the Parameters in Table 3

$\beta$	$[(\beta_{xxx} + \beta_{xyy} + \beta_{xzz})^2 + (\beta_{yyy} + \beta_{xyx} + \beta_{yzz})^2 + (\beta_{zzz} + \beta_{xxx} + \beta_{yyz})^2]^{1/2}$
$\alpha$	$1/3 (\alpha_{xx} + \alpha_{yy} + \alpha_{zz})$
$\mu$	$[(\mu_x)^2 + (\mu_y)^2 + (\mu_z)^2]^{1/2}$
$\chi$	$-1/2(E_{\text{HOMO}} + E_{\text{LUMO}})$
$\eta$	$-1/2(E_{\text{HOMO}} - E_{\text{LUMO}})$
$\sigma$	$1/\eta$

One of the most widely used methods to enhance average polarizability and first hyperpolarizability to the desired level is to select appropriate electron-donor and -acceptor pairs. When the results are analysed, it can be seen that the modifications in the triazene groups did not have a significant effect on these results ( $\beta_{(\text{tot})} = 117.854 \times 10^{-30} - 119.389 \times 10^{-30}$  esu;  $\alpha_{(\text{tot})} = 82.069 - 90.972 \times 10^{-24}$  esu). However, the designed homoconjugated systems give very similar NLO responses to  $\pi$ -conjugated push-pull structures in the literature.<sup>31,32</sup> These results indicate that homoconjugated systems can be used as an alternative to  $\pi$ -conjugated systems in NLO applications. Similarly, no significant differences were obtained in the parameters of electronegativity ( $\chi$ ), global chemical hardness ( $\eta$ ) and global softness ( $\sigma$ ) due to similar band-gap values calculated for chromophores ( $\pm$ )-**3a–e**. The promising results obtained in the NLO calculations led us to seek more detailed information about the structure. Since NLO measurements utilize lasers, the thermal stability requirement of push-pull chromophores is critical for NLO applications.<sup>33</sup> Compound ( $\pm$ )-**3a** was selected for thermogravimetric analysis (TGA) (Figure 3).

**Table 3** The Average Polarizability [ $\alpha_{(\text{tot})}$ ], First Hyperpolarizability [ $\beta_{(\text{tot})}$ ], Electric Dipole Moment  $\mu$  (D),  $E_{\text{HOMO}}$ ,  $E_{\text{LUMO}}$ ,  $\Delta E$  ( $E_{\text{HOMO}} - E_{\text{LUMO}}$ ), Electronegativity ( $\chi$ ), Global Chemical Hardness ( $\eta$ ), Global Softness ( $\sigma$ ) at the CAM-B3LYP/6-31G\* Level of Theory in  $\text{CH}_2\text{Cl}_2$

	( $\pm$ )- <b>3a</b>	( $\pm$ )- <b>3b</b>	( $\pm$ )- <b>3c</b>	( $\pm$ )- <b>3d</b>	( $\pm$ )- <b>3e</b>
$\alpha_{(\text{tot})}$ ( $\times 10^{-24}$ esu)	82.069	86.546	90.972	82.892	84.921
$\beta_{(\text{tot})}$ ( $\times 10^{-30}$ esu)	117.854	117.868	118.018	118.601	119.389
$\mu$ (D)	13.4790	13.5847	13.5290	13.9283	13.4642
$E_{\text{HOMO}}$ (eV)	-6.39	-6.38	-6.39	-6.38	-6.41
$E_{\text{LUMO}}$ (eV)	-4.09	-4.08	-4.09	-4.08	-4.10
$\Delta E$ (eV)	2.30	2.30	2.30	2.30	2.31
$\chi$ (eV)	5.24	5.23	5.24	5.23	5.26
$\eta$ (eV)	1.15	1.15	1.15	1.15	1.16
$\sigma$ (eV <sup>-1</sup> )	0.87	0.87	0.87	0.87	0.87

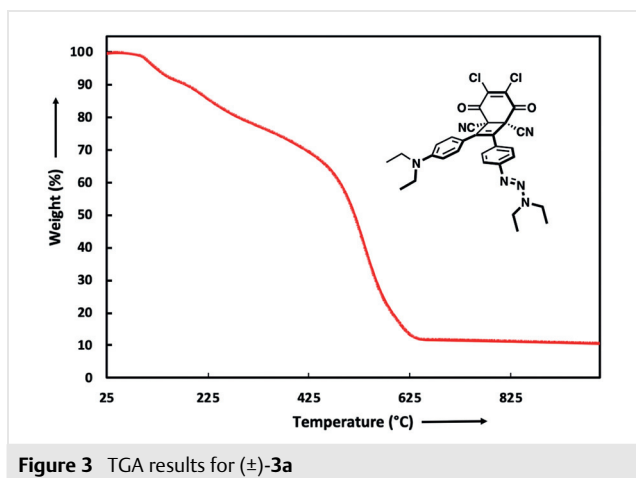


**Figure 3** TGA results for (±)-3a

Thermal decomposition of (±)-3a started at 100 °C and continued up to 640 °C. Considering that good thermal stability is considered to be resistance to temperatures above 300 °C, (±)-3a showed rather early thermal degradation. This is another reason why we have not performed experimental NLO measurements for chromophores (±)-3a-e.

In conclusion, five different homoconjugated push-pull chromophores were successfully synthesized by a click-type formal [2+2] cycloaddition in 51–65% yields. The optical and non-linear optical properties of the synthesized compounds were investigated in detail both experimentally and computationally. Accordingly, chromophores (±)-3a-e were found to have remarkable first-hyperpolarizability values and ground-state dipole moments. With the knowledge gained in this study, we continue to work on thermally more durable structures with superior NLO properties.

All reagents were purchased as reagent grade and used without further purification. Compounds 1a-e were prepared according to reported procedures.<sup>11</sup> Solvents for extraction or column chromatography were distilled before use. Reactions under exclusion of air or water were performed in oven-dried glassware and under argon or N<sub>2</sub> atmosphere. Column chromatography (CC) was carried out using SiO<sub>2</sub>-60 mesh. Analytical thin-layer chromatography (TLC) was performed on aluminum sheets or glass plates coated with 0.2 mm silica gel 60 F254; visualization with a UV lamp (254 or 366 nm). Evaporation *in vacuo* was performed at 25–60 °C and 900–10 mbar. Reported yields refer to spectroscopically and chromatographically pure compounds that were dried under high vacuum (0.1–0.05 mbar) before analytical characterization. <sup>1</sup>H and <sup>13</sup>C nuclear magnetic resonance (NMR) spectra were recorded at 400 MHz (<sup>1</sup>H) and 100 MHz (<sup>13</sup>C), respectively. Chemical shifts (δ) are reported in ppm downfield from tetramethylsilane using the residual deuterated solvent signal as an internal reference (CDCl<sub>3</sub>: δ<sub>H</sub> = 7.26 ppm, δ<sub>C</sub> = 77.0 ppm). For <sup>1</sup>H NMR spectra, coupling constants *J* are given in Hz, and the resonance multiplicity is described as s (singlet), d (doublet), t (triplet), q (quartet), and m (multiplet). All spectra were recorded at 298 K. The signal broadening and differentiation observed in the <sup>1</sup>H and <sup>13</sup>C NMR spectra are due to the restricted rotation of the N–N bond in the triazines.

High-resolution mass spectrometry (HRMS) was performed by the MS service of the Central Laboratory at Middle East Technical University, Turkey. Masses are reported in *m/z* units of the molecular ion as [M + H]<sup>+</sup>.

#### Synthesis of (±)-3a-e; General Procedure

A solution of 1a-e (1.5 mmol, 1 equiv) and DDQ (2) (1.5 mmol, 1 equiv) in CH<sub>2</sub>Cl<sub>2</sub> (8 mL) was stirred at 25 °C until complete consumption of starting material as based on TLC analysis. After evaporation of the solvent, products (±)-3a-e were purified by column chromatography (CC) (SiO<sub>2</sub>; CH<sub>2</sub>Cl<sub>2</sub>) and were obtained in 51–65% yields.

#### Compound (±)-3a

Yield: 52%; dark-brown solid; mp 124–126 °C (decomp.); *R<sub>f</sub>* = 0.64 (SiO<sub>2</sub>; CH<sub>2</sub>Cl<sub>2</sub>).

<sup>1</sup>H NMR (400 MHz, CDCl<sub>3</sub>, 298 K): δ = 7.50 (quasi d, *J* = 8.5 Hz, 2 H), 7.58 (quasi d, *J* = 9.0 Hz, 2 H), 7.44 (quasi d, *J* = 8.5 Hz, 2 H), 6.60 (quasi d, *J* = 9.0 Hz, 2 H), 3.80 (q, *J* = 7.0 Hz, 4 H), 3.40 (q, *J* = 6.9 Hz, 4 H), 1.23–1.36 (m, 6 H), 1.13–1.23 (m, 6 H).

<sup>13</sup>C NMR (100 MHz, CDCl<sub>3</sub>, 298 K): δ = 178.3, 177.4, 153.0, 149.8, 142.5, 142.0, 139.5, 133.2, 129.0, 127.8, 126.0, 121.2, 115.4, 112.7, 112.6, 111.3, 53.7, 53.4, 49.2, 44.7, 41.5, 14.4, 12.7, 11.5.

HRMS: *m/z* [M + H]<sup>+</sup> calcd for C<sub>30</sub>H<sub>29</sub>Cl<sub>2</sub>N<sub>6</sub>O<sub>2</sub><sup>+</sup>: 575.1729; found: 575.1732.

#### Compound (±)-3b

Yield: 61%; dark-brown solid; mp 120–122 °C (decomp.); *R<sub>f</sub>* = 0.62 (SiO<sub>2</sub>; CH<sub>2</sub>Cl<sub>2</sub>).

<sup>1</sup>H NMR (400 MHz, CDCl<sub>3</sub>, 298 K): δ = 7.58 (quasi d, *J* = 8.6 Hz, 2 H), 7.51 (quasi d, *J* = 9.0 Hz, 2 H), 7.45 (quasi d, *J* = 8.6 Hz, 2 H), 6.61 (quasi d, *J* = 9.0 Hz, 2 H), 5.34 (br. s, 1 H), 4.03 (br. s, 1 H), 3.40 (q, *J* = 7.1 Hz, 4 H), 1.18–1.40 (m, 18 H).

<sup>13</sup>C NMR (100 MHz, CDCl<sub>3</sub>, 298 K): δ = 178.3, 177.5, 153.5, 149.7, 142.5, 142.0, 139.2, 133.4, 128.9, 127.8, 125.6, 121.0, 115.4, 112.7, 112.6, 111.3, 53.7, 53.4, 49.4, 46.7, 44.7, 24.0, 19.5, 12.7.

HRMS: *m/z* [M + H]<sup>+</sup> calcd for C<sub>32</sub>H<sub>33</sub>Cl<sub>2</sub>N<sub>6</sub>O<sub>2</sub><sup>+</sup>: 603.2042; found: 603.2040.

#### Compound (±)-3c

Yield: 51%; dark-brown solid; mp 112–114 °C (decomp.); *R<sub>f</sub>* = 0.68 (SiO<sub>2</sub>; CH<sub>2</sub>Cl<sub>2</sub>).

<sup>1</sup>H NMR (400 MHz, CDCl<sub>3</sub>, 298 K): δ = 7.57 (quasi d, *J* = 8.6 Hz, 2 H), 7.50 (quasi d, *J* = 9.1 Hz, 2 H), 7.43 (quasi d, *J* = 8.6 Hz, 2 H), 6.60 (quasi d, *J* = 9.1 Hz, 2 H), 3.73 (t, *J* = 6.6 Hz, 4 H), 3.40 (q, *J* = 7.0 Hz, 4 H), 1.64–1.67 (m, 4 H), 1.34–1.40 (m, 4 H), 1.19 (t, *J* = 7.0 Hz, 6 H), 0.96 (t, *J* = 7.3 Hz, 6 H).

<sup>13</sup>C NMR (100 MHz, CDCl<sub>3</sub>, 298 K): δ = 178.3, 177.4, 153.0, 149.7, 142.5, 142.0, 139.3, 133.1, 128.9, 127.7, 125.8, 121.1, 115.3, 112.7, 112.6, 111.3, 54.7, 53.6, 53.4, 46.9, 44.7, 31.1, 28.2, 20.7, 20.0, 14.0, 12.7.

HRMS: *m/z* [M + H]<sup>+</sup> calcd for C<sub>34</sub>H<sub>37</sub>Cl<sub>2</sub>N<sub>6</sub>O<sub>2</sub><sup>+</sup>: 631.2355; found: 631.2355.

#### Compound (±)-3d

Yield: 56%; dark-brown solid; mp 118–120 °C (decomp.); *R<sub>f</sub>* = 0.24 (SiO<sub>2</sub>; CH<sub>2</sub>Cl<sub>2</sub>).



$^1\text{H}$  NMR (400 MHz,  $\text{CDCl}_3$ ):  $\delta$  = 7.57 (quasi d,  $J$  = 8.6 Hz, 2 H), 7.50 (quasi d,  $J$  = 9.1 Hz, 2 H), 7.43 (quasi d,  $J$  = 8.6 Hz, 2 H), 6.60 (quasi d,  $J$  = 9.1 Hz, 2 H), 3.95 (br. s, 2 H), 3.68 (br. s, 2 H), 3.40 (q,  $J$  = 7.0 Hz, 4 H), 2.05 (br. s, 4 H), 1.19 (t,  $J$  = 7.0 Hz, 6 H).

$^{13}\text{C}$  NMR (101 MHz,  $\text{CDCl}_3$ ):  $\delta$  = 178.1, 177.3, 153.1, 149.6, 142.4, 141.9, 139.3, 133.0, 128.8, 127.6, 125.9, 121.0, 115.2, 112.6, 112.5, 111.2, 53.5, 53.3, 51.3, 46.6, 44.5, 23.9, 12.5.

HRMS:  $m/z$  [ $M + H$ ] $^+$  calcd for  $\text{C}_{30}\text{H}_{27}\text{Cl}_2\text{N}_6\text{O}_2^+$ : 573.1573; found: 573.1568.

### Compound ( $\pm$ )-3e

Yield: 65%; dark-brown solid; mp 122–124 °C (decomp.);  $R_f$  = 0.66 ( $\text{SiO}_2$ ;  $\text{CH}_2\text{Cl}_2$ ).

$^1\text{H}$  NMR (400 MHz,  $\text{CDCl}_3$ , 298 K):  $\delta$  = 7.58 (quasi d,  $J$  = 8.6 Hz, 2 H), 7.50 (quasi d,  $J$  = 9.0 Hz, 2 H), 7.45 (quasi d,  $J$  = 8.6 Hz, 2 H), 6.60 (quasi d,  $J$  = 9.0 Hz, 2 H), 3.80–3.85 (m, 4 H), 3.40 (q,  $J$  = 7.1 Hz, 4 H), 1.70–1.75 (m, 6 H), 1.19 (t,  $J$  = 7.1 Hz, 6 H).

$^{13}\text{C}$  NMR (100 MHz,  $\text{CDCl}_3$ , 298 K):  $\delta$  = 178.2, 177.4, 152.6, 149.8, 142.5, 142.0, 139.7, 133.0, 129.0, 127.8, 126.4, 121.2, 115.3, 112.7, 112.6, 111.3, 53.7, 53.4, 44.7, 38.0, 31.1, 25.5, 24.4, 14.7, 12.7.

HRMS:  $m/z$  [ $M + H$ ] $^+$  calcd for  $\text{C}_{31}\text{H}_{29}\text{Cl}_2\text{N}_6\text{O}_2^+$ : 587.1729; found: 587.1724.

### Conflict of Interest

The authors declare no conflict of interest.

### Funding Information

This work was supported by Türkiye Bilimsel ve Teknolojik Araştırma Kurumu (TUBITAK) under the grant no. 218Z126. CD also acknowledges the financial support provided by the GEBIP Award of the Turkish Academy of Sciences.

### Acknowledgment

The authors would like to thank Esin Yaşar for the preparation of the graphical abstract.

### Supporting Information

Supporting information for this article is available online at <https://doi.org/10.1055/a-2004-6344>.

### References

- Kolb, H. C.; Finn, M. G.; Sharpless, K. B. *Angew. Chem. Int. Ed.* **2001**, *40*, 2004.
- Rostovtsev, V. V.; Green, L. G.; Fokin, V. V.; Sharpless, K. B. *Angew. Chem. Int. Ed.* **2002**, *41*, 2596.
- Tornøe, C. W.; Christensen, C.; Meldal, M. *J. Org. Chem.* **2002**, *67*, 3057.
- Michinobu, T.; Diederich, F. *Angew. Chem. Int. Ed.* **2018**, *57*, 3552.
- Lowe, A. B. *Polym. Chem.* **2010**, *1*, 17.
- Northrop, B. H.; Coffey, R. N. *J. Am. Chem. Soc.* **2012**, *134*, 13804.
- Hein, C. D.; Liu, X. M.; Wang, D. *Pharm. Res.* **2008**, *25*, 2216.
- Chen, G.; Qiu, Z.; Tan, J. H.; Chen, W. C.; Zhou, P.; Xing, L.; Ji, S.; Qin, Y.; Zhao, Z.; Huo, Y. *Dyes Pigm.* **2021**, *184*, 108754.
- Devibala, P.; Dheepika, R.; Vadivelu, P.; Nagarajan, S. *Chemistry-Select* **2019**, *4*, 2339.
- Malytskyi, V.; Simon, J. J.; Patrone, L.; Raimundo, J. M. *RSC Adv.* **2015**, *5*, 354.
- Mammadova, F.; Inyurt, F. C.; Barsella, A.; Dengiz, C. *Dyes Pigm.* **2023**, *209*, 110894.
- Hoffmann, R.; Woodward, R. B. *J. Am. Chem. Soc.* **1965**, *87*, 2046.
- Reinhoudt, D. N.; Kouwenhoven, C. G. *Tetrahedron* **1974**, *30*, 2093.
- Reinhoudt, D. N. *Adv. Heterocycl. Chem.* **1977**, *21*, 253.
- Dengiz, C.; Swager, T. M. *Synlett* **2017**, 28.
- Walker, D.; Hiebert, J. D. *Chem. Rev.* **1967**, *67*, 153.
- Kato, S. I.; Beels, M. T. R.; La Porta, P.; Schweizer, W. B.; Boudon, C.; Gisselbrecht, J. P.; Biaggio, I.; Diederich, F. *Angew. Chem. Int. Ed.* **2010**, *49*, 6207.
- Trofimov, B. A.; Sobenina, L. N.; Stepanova, Z. V.; Ushakov, I. A.; Sinogovskaya, L. M.; Vakulskaya, T. I.; Mikhaleva, A. I. *Synthesis* **2010**, 470.
- Erden, K.; Savaş, İ.; Dengiz, C. *Tetrahedron Lett.* **2019**, *60*, 1982.
- Frisch, M. J.; Trucks, G. W.; Schlegel, H. B.; Scuseria, G. E.; Robb, M. A.; Cheeseman, J. R.; Scalmani, G.; Barone, V.; Mennucci, B.; Petersson, G. A.; Nakatsuji, H.; Caricato, M.; Li, X.; Hratchian, H. P.; Izmaylov, A. F.; Bloino, J.; Zheng, G.; Sonnenberg, J. L.; Hada, M.; Fox, D. J.; Frisch, M. J.; Trucks, G. W.; Schlegel, H. B.; Scuseria, G. E.; Robb, M. A.; Cheeseman, J. R.; Scalmani, G.; Barone, V.; Mennucci, B.; Petersson, G. A.; Nakatsuji, H.; Caricato, M.; Li, X.; Hratchian, H. P.; Izmaylov, A. F.; Bloino, J.; Zheng, G.; Sonnenberg, J. L.; Hada, M.; Ehara, M.; Toyota, K.; Fukuda, R.; Hasegawa, J.; Ishida, M.; Nakajima, T.; Honda, Y.; Kitao, O.; Nakai, H.; Vreven, T.; Montgomery, Jr. J. A.; Peralta, J. E.; Ogliaro, F.; Bearpark, M.; Heyd, J. J.; Brothers, E.; Kudin, K. N.; Staroverov, V. N.; Kobayashi, R.; Normand, J.; Raghavachari, K.; Rendell, A.; Burant, J. C.; Iyengar, S. S.; Tomasi, J.; Cossi, M.; Rega, N.; Millam, J. M.; Klene, M.; Knox, J. E.; Cross, J. B.; Bakken, V.; Adamo, C.; Jaramillo, J.; Gomperts, R.; Stratmann, R. E.; Yazyev, O.; Austin, A. J.; Cammi, R.; Pomelli, C.; Ochterski, J. W.; Martin, R. L.; Morokuma, K.; Zakrzewski, V. G.; Voth, G. A.; Salvador, P.; Dannenberg, J. J.; Dapprich, S.; Daniels, A. D.; Farkas, Ö.; Foresman, J. B.; Ortiz, J. V.; Cioslowski, J.; Fox, D. J. *Gaussian 09*; Gaussian Inc: Wallingford, **2013**.
- Lee, C.; Yang, W.; Parr, R. G. *Phys. Rev. B* **1988**, *37*, 785.
- Cossi, M.; Rega, N.; Scalmani, G.; Barone, V. *J. Comput. Chem.* **2003**, *24*, 669.
- Runge, E.; Gross, E. K. U. *Phys. Rev. Lett.* **1984**, *52*, 997.
- Jödicke, C. J.; Lüthi, H. P. *J. Am. Chem. Soc.* **2003**, *125*, 252.
- Lokhande, P. K. M.; Patil, D. S.; Kadam, M. M.; Sekar, N. *Chemistry-Select* **2019**, *4*, 10033.
- Dengiz, Ç. *Turk. J. Chem.* **2021**, *45*, 1375.
- Erden, K.; Dengiz, C. *J. Org. Chem.* **2022**, *87*, 4385.
- Durand, R. J.; Achelle, S.; Gauthier, S.; Cabon, N.; Ducamp, M.; Kahlal, S.; Saillard, J. Y.; Barsella, A.; Robin-Le Guen, F. *Dyes Pigm.* **2018**, *155*, 68.
- Durand, R. J.; Achelle, S.; Robin-Le Guen, F.; Caytan, E.; Le Poul, N.; Barsella, A.; Guevara Level, P.; Jacquemin, D.; Gauthier, S. *Dalton Trans.* **2021**, 4623.
- Islam, N.; Chimni, S. S. *Comput. Theor. Chem.* **2016**, *1086*, 58.
- Solanke, P.; Achelle, S.; Cabon, N.; Pytela, O.; Barsella, A.; Caro, B.; Robin-le Guen, F.; Podlesný, J.; Klikar, M.; Bureš, F. *Dyes Pigm.* **2016**, *134*, 129.

- (32) Moshkina, T. N.; Le Poul, P.; Barsella, A.; Pytela, O.; Bureš, F.; Robin-Le Guen, F.; Achelle, S.; Nosova, E. V.; Lipunova, G. N.; Charushin, V. N. *Eur. J. Org. Chem.* **2020**, 5445.
- (33) Pan, Q.; Fang, C.; Li, F.; Zhang, Z.; Qin, Z.; Wu, X.; Gu, Q.; Yu, J. *Mater. Res. Bull.* **2002**, 37, 523.